

Thin Film Materials Exposure to Low Earth Orbit Aboard Space Shuttle

R. A. Synowicki,* Jeffrey S. Hale,[†] Blaine Spady, Mike Reiser,[†] S. Nafis,[‡] and John A. Woollam[§]
University of Nebraska, Lincoln, Nebraska 68588-0511

To study the effects of Atomic Oxygen on various thin film materials, fourteen thin film samples were exposed to the corrosive environment of low Earth orbit. Total exposure was 42 hours, resulting in a nominal atomic oxygen fluence of 2.2×10^{20} atoms/cm². The films included aluminum, diamondlike carbon, diamond, and multi-layer stacks. Included are experimental details of sample preparation, exposure, and post-flight results. Pre-flight characterization techniques included Variable Angle Spectroscopic Ellipsometry, optical reflectance and transmittance, Atomic Force Microscopy, and Raman scattering. Post-flight analysis repeated pre-flight characterization. Aluminum films resisted degradation. Surface contaminants were identified using Auger Electron Spectroscopy. Contaminants were SiO₂, fluorine, and sulfur which most likely result from degradation of cargo bay lining, waste water dumps, and outgassing. Diamondlike carbon films were completely etched away during exposure. Polycrystalline diamond films were extremely resistant to atomic oxygen degradation, showing no post-flight structural, compositional, or mass changes. Aluminum films 23.5 nm thick simultaneously protect silver reflecting layers from oxidation and increase the ultraviolet reflectance of the stack. Decreasing the aluminum thickness to 7.5 nm resulted in complete oxidation during exposure and failure as a protective coating.

Introduction

THE Center for Microelectronic and Optical Materials Research (CMOMR) prepared and characterized twenty samples of candidate spacecraft materials for low Earth orbit (LEO) durability studies. The samples were flown aboard shuttle flight Space Transportation System (STS)-46 on Limited Duration space environment Candidate materials Exposure payload (LDCE)-2 and 3. The samples were exposed to ram Atomic Oxygen (AO) in LEO for 42 hours to a nominal fluence of 2.2×10^{20} atoms/cm². These samples included thin films of aluminum, diamondlike carbon, diamond, and optical multilayer stacks. Included also were bulk samples of graphite, carbon/boron nitride, and carbon/carbon composites. However, this paper will focus on the thin film samples only. Results for the bulk materials will be presented in a separate paper.

This paper presents a summary of sample selection, preparation, characterization, and mounting for space flight. Post-flight experimental results are presented for the thin film samples. When applicable, results are compared to laboratory simulations using oxygen plasma ashers.

STS-46 Flight Profile

The predicted atmospheric concentration of oxygen and nitrogen during the forty hours of exposure at an orbital altitude of 241 km (130 nautical miles) was predicted by NASA prior to the flight. When the orbital position and velocity of the shuttle, as well as solar and geomagnetic activity were taken into account, the incident particle fluxes were calculated. These are shown in Fig. 1. Figure 2 shows the total atomic oxygen fluence for various exposure angles predicted as a function of time. The predicted pre-flight AO fluence was determined to be 2×10^{20} atoms/cm². These figures were calculated using the Mass Spectrometer Incoherent Scatter (MSIS)-86 Thermospheric model.¹

The samples were exposed along the ram direction to maximize atomic oxygen exposure. The ram direction is defined as the direction parallel to the shuttle velocity vector (or normal to the sample

surface for this experiment.) The total ram AO fluence was measured between 2.0×10^{20} and 2.5×10^{20} oxygen atoms/cm² by a mass spectrometer flown on the Evaluation of Oxygen Interaction with Materials payload (EOIM)-III mission payload.² Kapton[®] polyimide was exposed on EOIM-III and used as an alternate method for fluence calibration. Kapton mass loss measurements determined the exposed fluence to be 2.3×10^{20} atoms/cm². EOIM-III was active during the same time period as the LDCE payloads. Post-flight modeling using MSIS-86 was performed using the actual exposure conditions during the flight (these apply equally well to both the EOIM and LDCE payloads). This post-flight modeling yielded a higher fluence of 2.2×10^{20} atoms/cm² due primarily to geomagnetic storms which occurred during the flight.² This dose is approximately equal to doses obtained in laboratory based plasma asher simulations after 6 to 7 hours.

Both the LDCE-2 and 3 payloads were placed into GAS (Get Away Special payload container for small experiments) cans and mounted against the back bulkhead (Bay 13) of the shuttle cargo bay. The LDCE-2 tray was exposed by the opening of a motorized door on orbit 94 of the mission at Mission Elapsed Time (MET) of 5 days, 22 hours, 41 minutes (5:22:41). This door was closed 42 hours later at 7:16:10 MET.² Samples in the LDCE-3 tray were exposed throughout the flight to the ambient environment, and received direct exposure to ram atomic oxygen during the same 42 hours that LDCE-2 was active. The first nine samples listed on Table 1 were included on the LDCE-2 tray, while the remainder were placed on the LDCE-3 tray.

Materials Chosen for Space Exposure

Table 1 lists the twenty samples exposed aboard STS-46, as well as the experimental techniques used to characterize the samples. Thin film coatings of aluminum can be used either as reflective surfaces in power systems, or as oxidation resistant coatings for spacecraft structural members and optical surfaces. The aluminum coating samples one through three in Table 1 were sputter deposited, while the coatings on samples four to six were electron beam evaporated. Using two distinctly different deposition methods allows for comparison of LEO effects as a function of deposition type.

Samples seven through ten were "Diamondlike" carbon (DLC) films of different thicknesses and optical gap. DLC films have been considered for impact resistant coatings due to the extreme hardness of these films.³ Samples 8 and 10 were deposited from methane in an argon plasma at University of Nebraska-Lincoln (UNL) by Plasma Enhanced Chemical Vapor Deposition (PECVD).⁴ Samples 7 and 9

Received Sept. 24, 1993; revision received Sept. 20, 1994; accepted for publication Sept. 23, 1994. Copyright © 1994 by the American Institute of Aeronautics and Astronautics, Inc. All rights reserved.

*Graduate Student, Department of Electrical Engineering. Member AIAA.

[†]Graduate Student, Department of Electrical Engineering.

[‡]Research Assistant Professor, Department of Electrical Engineering.

[§]Director, Center for Microelectronic and Optical Materials Research.

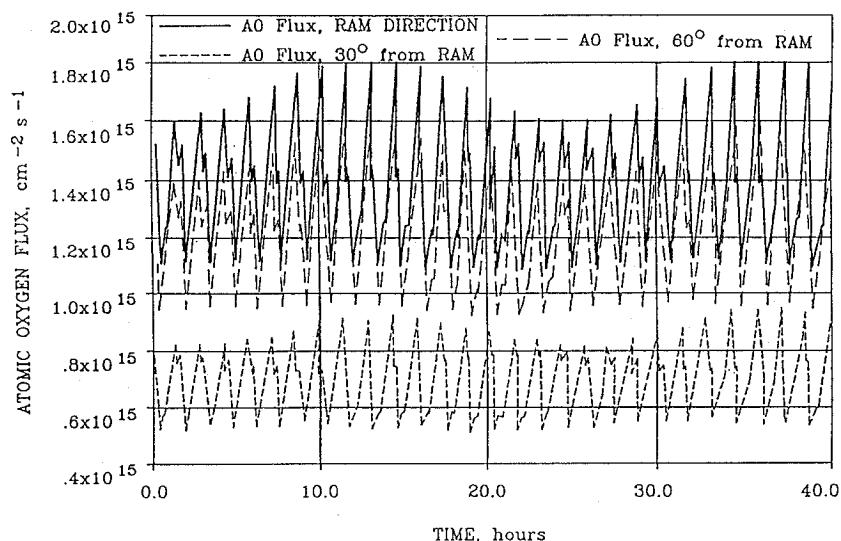


Fig. 1 Predicted STS-46 atomic oxygen flux as a function of angle for 40 hours of space exposure: altitude = 130 n.mi., inclination = 28.5 deg.

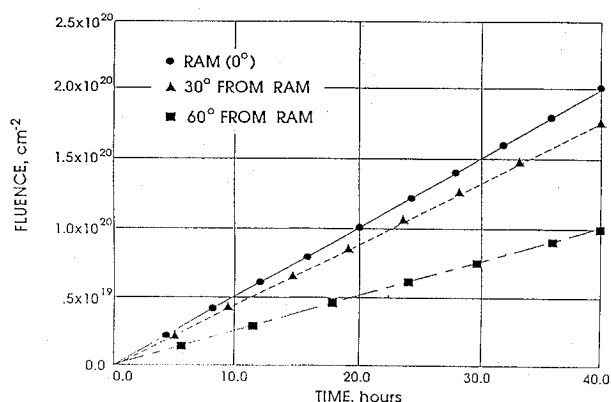


Fig. 2 Predicted atomic oxygen fluence as a function of angle for exposure on STS-46: altitude = 130 n.mi., inclination = 28.5 deg.

were deposited by chemical vapor deposition (CVD) at the NASA-Lewis Research Center.

The authors propose that DLC films be used as a degradation standard for LEO simulations in the laboratory as well as on orbital exposures. Diamondlike films could provide more accurate fluence measurements than currently used samples of Kapton polyimide since these films are not affected by environmental factors such as moisture absorption.^{4,5} Also, the erosion depth of Kapton is usually measured by stylus profilometry. Since Kapton presents a rough surface after exposure to directed AO, uncertainty is added to calculations of eroded sample volume.

With thin films of DLC, thickness erosion as a function of fluence can be calibrated more accurately than with Kapton since films remain smooth after directed AO exposure, allowing for thickness changes to be accurately measured by optical methods. Reflectance spectrophotometry and ellipsometry are well suited to this purpose. Mass loss and film thickness loss allow for two separate measurements of fluence using a single DLC film, one physical through sample mass loss, the other optical through measured changes in film thickness. However, it will be shown that the erosion rate of DLC is very high, making it only useful for low fluence exposures.

Polycrystalline diamond films show potential as protective layers for spacecraft components due to their extreme hardness, optical properties, and thermal conductivity. Samples 11 and 12 on Table 1 are thin films of polycrystalline diamond which were deposited using hot filament and plasma CVD techniques. These films contain both crystalline diamond as well as graphite. Changes in the relative amounts of each component due to atomic oxygen exposure can be measured with Raman scattering.⁶

Table 1 Materials exposed aboard shuttle flight STS-46 with types of data acquired

Description	a	b	c	d	e	f	g
70 nm Al/Quartz	X	X	X	X	X		
100 nm Al/Quartz	X	X	X	X	X		
150 nm Al/Quartz	X	X	X	X	X		
70 nm Al/Quartz	X	X	X	X	X		
100 nm Al/Quartz	X	X	X	X	X		
150 nm Al/Quartz	X	X	X	X	X		
500 nm DLC/Quartz		X		X	X		
100 nm DLC/Quartz		X	X	X	X		
500 nm DLX/Si	X	X	X	X	X		
1000 nm DLC/Si	X	X	X	X	X		
Diamond/Quartz		X		X	X		X
Diamond/Quartz		X		X	X		X
Solar Concentrator Multilayer	X	X		X	X		
Solar Concentrator Multilayer	X	X		X	X		
Pyrolytic Graphite Highly Oriented	X	X		X	X	X	
Pyrolytic Graphite 40% C/BN		X		X	X	X	
60% C/BN	X	X		X	X	X	
Graphite C/C Composite		X		X	X	X	
Graphite C/C Composite		X		X	X	X	

a. Variable Angle Spectroscopic Ellipsometry

b. Photography

c. Atomic Force Microscopy

d. Spectrophotometry

e. Mass and Dimensions

f. Scanning Electron Microscopy

g. Raman Scattering

Samples 13 and 14 are thin film multilayer stacks that have been sputter deposited onto T-300/934 graphite-epoxy substrates. The layer structure is shown in Fig. 3. The films consist of a 100 nm thick copper adhesion promoting layer between the graphite-epoxy substrate and a silver reflecting layer. The 100 nm thick silver reflecting layer is protected from oxidation by a thin film of aluminum 7.5 or 23.5 nm thick, and a layer of SiO₂ approximately 90 nm thick. Multilayer stacks of this type have been considered for solar dynamic power system concentrators.⁷ The aluminum layer is less than optically thick and serves as a sacrificial barrier to atomic oxygen. The aluminum layer also serves to enhance the ultraviolet reflectance of the stack since the plasma edge of silver occurs near 320 nm where reflectance falls quickly to 22%. The plasma edge of

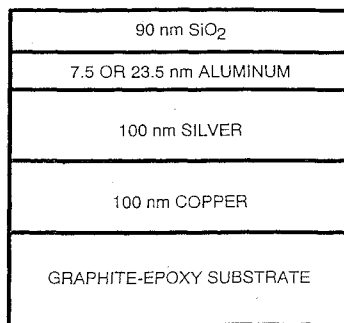


Fig. 3 Construction of multilayer film stack.

aluminum occurs at far higher energy, insuring good reflectance at wavelengths well below 320 nm.⁸

Experimental Techniques

Experimental techniques used for pre-flight characterization are limited to nondestructive techniques. Variable Angle Spectroscopic Ellipsometry (VASE®)^{9,10,11} was used to determine layer thicknesses, composition, and surface oxidation for the films. VASE was not used for samples of diamondlike carbon/quartz because back-surface reflections from the quartz substrate were not analyzable at the time this research was done. Also, diamond films are too rough to be analyzed using VASE.

Surface photography of all samples was used to characterize macroscopic surface topography. Photographs were taken through a Nomarski optical interference contrast microscope under a variety of lighting and filtering conditions. Each sample was carefully positioned within a custom-made holder which insures that the same area is photographed during post-flight analysis. Macroscopic changes in surface topography result primarily from micrometeoroid impacts, although cracking may occur as a result of thermal cycling, and surface texturing from directed AO attack.

Atomic force Microscopy was used for microstructural surface characterization of all aluminum and diamondlike carbon films. Changes in topography due to surface oxidation and/or contamination of the aluminum films were investigated and these results compared with ground-based LEO simulations.²

All samples were characterized by reflectance spectrophotometry. Specular transmission measurements were also performed on transparent samples. Losses in reflectance and transmittance of thin film samples are related to surface roughness, surface contamination, and/or changes in the electronic structure of the material.

The physical dimensions of all samples were measured with a Vernier caliper. Masses were measured with an ultramicrobalance with resolution of 10^{-7} g. Accurate mass loss measurements are required to determine the erosion rate and erosion yield of a particular material.

Finally, diamond thin film samples were characterized by Raman scattering. Raman data was used to measure changes in the relative amounts of diamond and graphite in the films. The diamond crystallites are sp³ bonded and are as stable as bulk diamond. However, the sp² bonded graphite component of the films is found at grain boundaries between the crystallites. Graphite is known to be readily etched in both LEO and laboratory simulations. It is quite possible, even expected, that LEO exposure preferentially etches the graphitic component of the films, with no effect on the diamond crystallites.

Preparation and Mounting of Samples

The most challenging engineering aspect of sample preparation was constructing samples that would fit properly into the provided holder. During launch, the Space Shuttle and payload are exposed to an acceleration of 4 g as well as extreme vibration. Secure mounting is required to prevent damage or even breakage, which could cause contamination or damage to other parts of the payload.

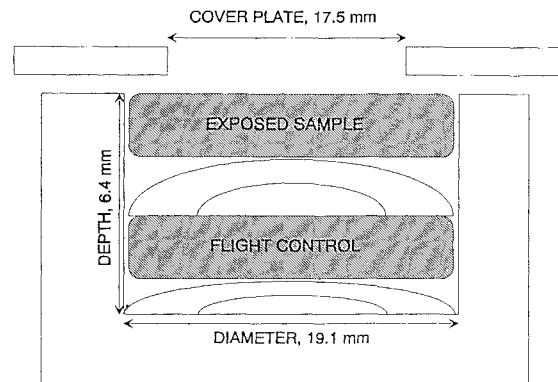


Fig. 4 Sample configuration used for LDCE-2 and 3.

Thin film samples were deposited onto either quartz or single crystal silicon substrates. After pre-flight characterization, the samples were integrated with the flight hardware.

For this study, two samples 1.59 mm (1/16 of an inch) thick, were placed atop each other into a single hole in the holder. This allowed for the lower sample to act as a flight control while the upper sample was exposed to ram atomic oxygen. This configuration is shown in Fig. 4. The exposed sample was separated from the control sample by a spacer or spring washer. The main reason for using such a configuration is that both the control and exposed samples were subjected to the same ground environment (humidity, temperature, etc.) before and after flight. However, due to the directional nature of atomic oxygen in orbit, the control sample was masked from direct atomic oxygen exposure. Both the exposed sample and the control sample were compared with additional control samples kept in the laboratory.

Results and Discussion

The pre- and post-flight sample masses are shown in Table 2. Note that the metallic thin film samples show no change in mass. The same is true for the diamond films. However, large mass changes are seen in the correctly-exposed (no chips or mounting problems) diamondlike carbon films as a result of etching by atomic oxygen.

The VASE analysis of the aluminum films is shown in Table 3. Note that all control samples show some oxide layer of growth of 1.1 to 1.9 nm due to aging. However, the space exposed samples show a larger increase in oxide thickness of up to 3.7 nm. It is useful to note that these films showed no change in specular reflectance after flight when measured with reflectance spectrophotometry. This is because changes in oxide thickness on this small scale are not observable using only reflected intensity measurements. However, ellipsometry was sensitive to these small oxide thickness changes since it measures changes in polarization rather than intensity.

When these results are compared to those using a plasma asher,¹² it is clear that LEO exposure induces additional oxide layer growth on the order of 1 to 2 nm, while films exposed to the same fluence in the asher show much smaller changes on the order of 0.3 nm.

Pre-flight and post-flight Atomic Force Microscopy (AFM) data show no significant changes in surface roughness with LEO exposure. This result differs with those obtained using ashers with contaminants present, where surface deposits were found to grow with ashing. However, when using an asher where contamination is nearly non-existent, these space-based results agree well with ashed aluminum films.

Auger electron spectroscopy was used to identify surface contaminants on the aluminum films. Figure 5 shows a surface scan of a space exposed aluminum film. Note the presence of large peaks at 51, 503, and 1396 eV, corresponding to Al₂O₃, oxygen, and elemental Al respectively. These three peaks are expected and result from the deposited film structure. The large peak at 272 eV is due to carbon, most of which results from handling and/or organics settling from the ambient air at ground level. However, some carbon can result from etching products settling onto the aluminum film surfaces, but these are indistinguishable from other carbon contaminants.

Table 2 Mass change after spaceflight exposure

Sample	Preflight, mg	Postflight, mg	Change, mg	Comments
70 nm Al	870.579	870.576	-0.003	Stable
100 nm Al	858.274	858.269	-0.005	Stable
150 nm Al	854.975	854.965	-0.010	Stable
70 nm Al	853.294	853.295	+0.001	Stable
100 nm Al	856.358	856.363	+0.005	Stable
150 nm Al	860.158	860.162	+0.004	Stable
500 nm DLC	873.860	Chipped	*	Sample chipped, data not accurate
100 nm DLC	837.804	837.790	-0.014	Sample not exposed
500 nm DLC	915.741	915.537	-0.204	Completely eroded
1000 nm DLC	729.278	729.006	-0.272	Completely eroded
Diamond	969.02	969.04	+0.02	Stable
Diamond	965.28	Broken	*	Broke after flight, no result
Multilayer	161.316	161.320	+0.004	Stable
Multilayer	155.781	155.795	+0.014	Stable

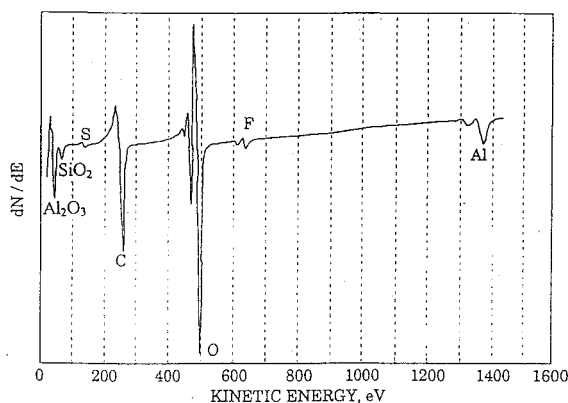


Fig. 5 Auger surface scan of an aluminum thin film after flight.

Peaks are also seen at approximately 76, 140, and 640 eV. The peak at 76 eV corresponds to deposited SiO_2 . Since Auger spectroscopy is sensitive to single layers (monolayers) of contaminant films, detection of elemental Aluminum and Al_2O_3 indicates that some sub-monolayer SiO_2 contaminant was deposited during flight exposure. The peaks at 140 and 640 eV correspond to sulfur and fluorine respectively. The presence of these SiO_2 , Fluorine, and Sulfur contaminants was not seen on the unexposed control samples.

The sources of the contaminants can never be known exactly, but some very likely sources can be identified.² The shuttle's cargo bay is lined with a white-colored thermal blanket material known as Beta Cloth. Beta Cloth is a composite made from a glass fiber weave impregnated with PTFE (Teflon). During manufacture, the glass weave is dusted with a thin layer of silicone based oil to improve handling. The oiled weave is then impregnated with the Teflon. The entire shuttle cargo bay, including the rear bulkhead nearest the samples is covered with Beta Cloth.

It is known that Teflon has a low, but nonzero erosion yield. Throughout LDCE activation, the shuttle cargo bay was facing into the ram direction, exposing the entire bay, payloads, and lining to atomic oxygen. Teflon erosion may also have been enhanced by the high Vacuum Ultraviolet radiation (VUV) fluence received during deployment of the EURECA satellite earlier in the mission. It is suspected that erosion products from the Beta Cloth (fluoropolymers and silicones) have settled onto the samples and result in the observed SiO_2 and fluorine contaminants. Any additional carbon attached to these etching products serves only to enhance the carbon peak at 272 eV.

Sulfur is indicated near 140 eV. There are two likely sources for this contaminant. First, ground handling at Kennedy Space Center might have some effect due to H_2S present in the environment. However, this seems unlikely since clean conditions are maintained as much as possible.

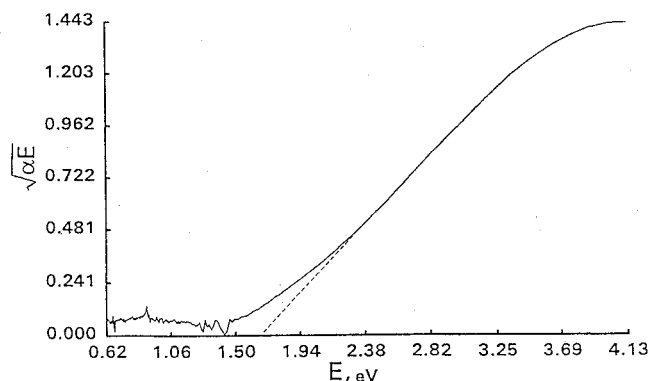


Fig. 6 Tauc plot of a diamondlike carbon thin film: band gap = 1.66 eV.

A second and more likely source of the sulfur contaminant are waste water dumps performed periodically during shuttle missions or outgassing of volatiles from the orbiter Waste Collection System. A waste water dump was performed on-orbit approximately two hours before LDCE-2 activation. The waste dump occurred at mission elapsed time of 5:20:37. The shuttle orientation was changed to put the cargo bay into the ram direction at 5:22:30 MET, and LDCE-2 activation followed at 5:22:41 MET.

The optical band gap of the DLC films was determined by measuring optical absorbance and fitting to the Tauc formula as shown in Fig. 6.¹³ The Tauc formula is defined as

$$\alpha E = \beta(E - E_g)^2$$

where α is the absorption coefficient of the film, E is the photon energy, β is a constant, and E_g is the optical band gap of the material. The quantity $(\alpha E)^{1/2}$ is plotted as a function of E to show the absorption edge as a linear region on the plots. The linear region is extrapolated to the E -axis intercept, which gives the optical band gap of the material. This method is valid since the diamondlike films are amorphous. The optical gap of films made at UNL averaged to 1.66 eV, while those supplied by NASA showed a band gap of 2.74 eV. The optical band gap is related to the hydrogen content of the films, which in turn is related to the hardness of the film. By exposing DLC samples with differing optical gap the effect of film hardness on erosion rate can be determined.

Three of the four diamondlike films exposed to LEO were found to have been eroded completely, leaving nothing but the bare substrate exposed. The fourth film was inadvertently mounted upside down in the holder and received effectively zero atomic oxygen fluence. The complete erosion of the films is unfortunate since it becomes impossible to precisely determine erosion rate via mass loss and film thickness. Since all films were completely eroded, no conclusions can be drawn regarding the effect of film hardness

on atomic oxygen resistance. This study will require further LEO exposure of diamondlike films and continued asher studies with thicker films. However, this null result does show that DLC should not be considered as a long-duration protective coating.

The diamond thin films exposed show no change in their composition. It was expected that the graphitic component of the films present at the grain boundaries would be preferentially etched by the atomic oxygen, leaving the diamond crystallites unharmed. The pre-flight and post-flight Raman spectroscopy data in Fig. 7 show no significant change in the graphitic component of the film above 1400 cm^{-1} . The diamond peak at 1330 cm^{-1} shows slight changes in amplitude, but this is associated with positioning of the sample for Raman analysis, and not a difference in film composition. Contaminants were not visible with Raman analysis because the technique is based on photon scattering from crystalline structures. The trace amounts of contaminants detected on the aluminum films with Auger spectroscopy could not coalesce into crystalline states.

The mass loss and optical data (absorbance) for the diamond films show no significant change. It seems clear that diamond is very resistant to the effects of LEO. This same result is also seen in ashers. Diamond films seem very promising for use as a spacecraft coatings. Unfortunately, at this time, films can be prepared only at temperatures greater than about 700°C , which severely limits the number of surfaces on which it can be deposited. Unlike the aluminum films, the diamond films were not screened for contamination with Auger analysis, although similar results could be expected.

The multilayer films of silver with overcoats of aluminum and SiO_2 gave very interesting and useful results. Ellipsometry was used to determine changes in thickness and composition of the metal and dielectric layers.

The multilayer containing aluminum 7.5 nm thick did not protect the silver reflector from oxidation. The silver reflective layer was nominally 100 nm thick, which is optically thick throughout the spectral range acquired. The aluminum layer was modeled using a mixture of elemental aluminum and Al_2O_3 via the Bruggeman Effective Medium Approximation (EMA), which assumes uniform, simple mixtures.¹⁴ Before flight, the thickness of the aluminum layer averaged to $7.5 \pm 0.2\text{ nm}$ with an average composition of $36.8 \pm 2.3\%$ Al_2O_3 . The pre-flight SiO_2 thickness averaged to $90.3 \pm 2.0\text{ nm}$. After flight, the control samples showed some aging. The aluminum layer thickness averaged to $7.4 \pm 0.5\text{ nm}$, which is nearly identical to the pre-flight thickness. However, the Al_2O_3 composition increased 5.5% to $42.3 \pm 1.2\%$. This aging is to be expected and is similar to results seen on the aluminum films tabulated in Table 3. This indicates that the 90 nm overlayer of SiO_2 is not serving to protect the aluminum and silver layers beneath. This probably results from nonuniformity of the graphite-epoxy surface, resulting in inadequate coverage of the SiO_2 film, and possibly microscopic cracking of the glassy film due to handling and thermal expansion.

The aluminum oxide layer formed during aging or flight exposure was not modeled as a pure Al_2O_3 layer over a thin aluminum film

Table 3 Oxide growth on aluminum films

	Film Thickness	Exposed Film Changes	Control Sample Changes
Sputtered	100 nm	2.2 nm	$1.2 \pm 0.5\text{ nm}$
	150 nm	2.1 nm	$1.1 \pm 0.2\text{ nm}$
Electron Beam	70 nm	3.0 nm	$1.5 \pm 0.4\text{ nm}$
	100 nm	3.5 nm	$1.6 \pm 0.2\text{ nm}$
Evaporated	150 nm	3.7 nm	$1.9 \pm 0.1\text{ nm}$

Notes: Ellipsometry used to measure oxide growth, and all values are changes in Al_2O_3 thickness.

because both oxide layers (SiO_2 and Al_2O_3) would have similar optical constants, resulting in significant parameter correlation between these two similar layers. Therefore, oxidation of the uppermost aluminum layers is absorbed into the EMA mixture as a compositional change.

The exposed flight sample showed significant change after exposure. The aluminum layer best fit to a thickness of 6.3 nm with an Al_2O_3 composition of 99.3%. The underlying silver layer showed oxidation to a depth of 7.1 nm with a composition of 81.3% Ag_2O . It is clear that the 7.5 nm thick aluminum layer was completely oxidized, allowing oxygen to reach the Al/Ag interface.

Increasing the thickness of the aluminum layer to 23.5 nm adequately protects the silver from oxidation. Pre flight analysis showed the aluminum layer thickness to be $23.5 \pm 3.0\text{ nm}$ with an aluminum oxide composition of $22.5 \pm 2.5\%$. The SiO_2 overcoat averaged to $91.2 \pm 1.8\text{ nm}$. Post-flight analysis of the control samples again showed aging effects due to inadequate protection from the SiO_2 overlayer. Aging caused the combined aluminum + Al_2O_3 layer thickness to increase by 6.2 nm to $29.7 \pm 2.8\text{ nm}$. The Al_2O_3 fraction also increased by 9.8% to $32.3 \pm 1.3\%$.

The exposed flight sample best fit a model containing a 23.8 nm thick aluminum layer with an Al_2O_3 composition of 38.6%. For this exposed film, the layer thickness did not change significantly after exposure, but the oxide composition increased by over 16%. Again, the oxidation of the uppermost layers of aluminum is absorbed into the EMA as a compositional change. Absolutely no Ag_2O was detected anywhere in the stack. In this case an aluminum film 23.5 nm thick adequately protects silver from oxidation.

Summary and Conclusions

Twenty samples of various thin film and bulk materials were prepared and launched aboard Space Shuttle flight STS-46. The samples were exposed to a nominal atomic oxygen fluence of 2.2×10^{20} atoms/ cm^2 during 42 hours of ram-directed exposure. The samples were characterized by nondestructive techniques including ellipsometry, atomic force microscopy, optical spectrophotometry, and Raman scattering.

Preparation of samples for mounting in the sample holder required great care and a precise fit because a shuttle launch may cause damage to sample surfaces. Control samples were flown along with exposed flight samples. This was accomplished by placing the control beneath the flight sample because atomic oxygen degradation is directional in nature.

Thin films of aluminum showed changes in oxide thickness on the order of 1 to 2 nm over unexposed films. Also, surface contaminants of SiO_2 , fluorine, and sulfur were deposited through LEO exposure. It is believed the SiO_2 and fluorine result from etching of the Beta Cloth lining of the shuttle cargo bay. The sulfur could be due to terrestrial H_2S , but most likely results from waste water dumps performed before exposure began or outgassing of waste volatiles.

Diamondlike carbon films exposed in orbit were completely etched away. This was unfortunate and does not allow for determination of on-orbit degradation rates. However, the very high erosion yield implied by this result shows that DLC should not be considered for an atomic oxygen protective coating.

The diamond films exposed show no changes in mass, optical properties or composition. This result indicates that diamond films are extremely resistant to LEO degradation and deserve further consideration for spacecraft application.

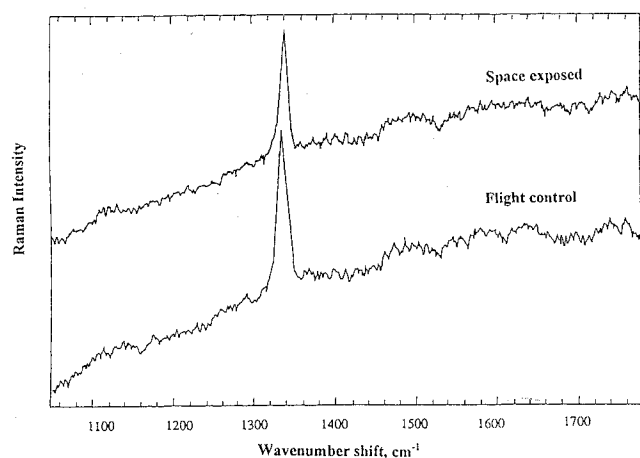


Fig. 7 Raman scans of two diamond films after flight.

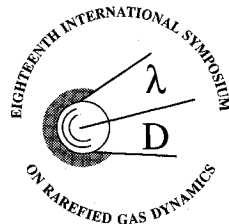
Thin films of aluminum were used effectively to prevent corrosion of silver reflecting surfaces. Aluminum films 7.5 nm thick were completely oxidized by LEO exposure, and were not thick enough to prevent significant oxidation of the underlying silver layer. However, a 23.5 nm thick film of aluminum remained far from fully oxidized and protected the silver layer from atomic oxygen degradation.

Acknowledgments

The authors extend thanks to NASA Lewis Research Center for funding this work under Grant NAG-3-95. The Nebraska Space Grant Consortium also contributed funding for student support on this project. The article reflects the work of many individuals who gave their time and resources to make this project complete. The authors would like to thank Rod Dillon and Hsuing Chen of the University of Nebraska-Lincoln Center for Microelectronic and Optical Materials Research (UNL CMOMR) for preparation and characterization of the polycrystalline diamond films studied in this work. Thanks to Ned Ianno of the UNL CMOMR for use of his diamondlike carbon deposition equipment, and to Carlos R. Morrison and Sam Alterovitz of NASA-Lewis for contributing diamondlike carbon films. Jim T. Visentine at Johnson Space Center was kind enough to allow reproduction of his predicted orbital fluences.

References

- ¹Hedin, A. E., "MSIS-86 Thermospheric Model," *Journal of Geophysical Research*, Vol. 92, No. A5, 1987, pp. 4649-4662.
- ²Synowicki, R. A., "Low Earth Orbit Degradation of Spacecraft Materials: Plasma Asher Simulation with Comparison to Spaceflight Exposure," M.S. Thesis, Univ. of Nebraska-Lincoln, NE, July 1993.
- ³Gulino, D. A., "Thin Film Coatings For Space Electrical Power System Applications," in *Surface Modification Technologies II*, edited by T. S. Sudarshan and D. G. Bhat, The Minerals Metals and Materials Society, 1989, pp. 73-90.
- ⁴Hale, J. S., Synowicki, R. A., Nafis, S., and Woollam, J. A., "Atomic Oxygen Plasma Effects on CVD Deposited Diamond-Like Carbon Films," *Materials Research Society*, Vol. 36, 1992, pp. 307-312.
- ⁵Rutledge, S. K., Banks, B. A., DiFilippo F. B., Joyce, D. T., and Hotes, D., *An Evaluation of Candidate Oxidation Resistant Materials for Space Applications in LEO*, NASA Tech. Memo. 100122, Nov. 1986.
- ⁶Brundle, R. C., Evans, C. A. Jr., and Wilson, S., *Encyclopaedia of Materials Characterization*, 1st ed., Butterworth-Heinemann, Boston, MA, 1992, pp. 428-441.
- ⁷DeGroh, K. K., Dever, T. M., and Quinn, W. F., *The Effect of Leveling Coatings on the Atomic Oxygen Durability of Solar Concentrator Surfaces*, NASA Tech. Memo. 102557, April 1990.
- ⁸Wooten, F., *Optical Properties of Solids*, 1st ed., Academic Press Inc., San Diego 1972, p. 59.
- ⁹Woollam, J. A., and Snyder, P. G., "Fundamentals and Applications of Variable Angle Spectroscopic Ellipsometry," *Mat. Sci. Eng.*, Vol. B5, Jan. 1990, pp. 279-283.
- ¹⁰Alterovitz, S. A., Woollam, J. A., and Snyder, P. G., "Variable Angle Spectroscopic Ellipsometry," *Solid State Technology*, Vol. 31, 1988, pp. 99-102.
- ¹¹Azzam, R. M. A., and Bashara, N. M., *Ellipsometry and Polarized Light*, 1st ed., North Holland, New York, 1977.
- ¹²Synowicki, R. A., Hale, J. S., McGahan, W. A., Ianno, N. J., and Woollam, J. A., "Oxygen Plasma Ashers as Space Simulators: A Quantitative Analysis of Contamination with Identification of Sources and Remedies," *Applied Physics Communications*, Vol. 12, No. 3-4, 1993, pp. 275-300.
- ¹³Smith, R. A., *Semiconductors*, 2nd ed., Cambridge Univ. Press, Cambridge, England, UK, 1978, pp. 483-499.
- ¹⁴Aspnes, D. E., Theeten, J. B., and Hottier, F., "Investigation of Effective Medium Models of Microscopic Surface Roughness by Spectroscopic Ellipsometry," *Phys. Rev. B*, Vol. 20, No. 8, Oct. 1979, pp. 3292-3302.



Rarefied Gas Dynamics

Bernie D. Shizgal, *University of British Columbia, Vancouver, British Columbia*; David P. Weaver, *Phillips Laboratory, Edwards Air Force Base, CA*, editors

These three volumes contain 168 technical papers presented in 44 sessions at the Eighteenth International Symposium on Rarefied Gas Dynamics, which took place at the University of British Columbia, Vancouver, British Columbia, Canada, July 26-30, 1992. Hundreds of figures accompany the reviewed and revised papers.

Traditional areas of kinetic theory, discrete velocity models, freejets, hypersonic and rarefied flows, shock phenomena, condensation and evaporation, and associated mathematical and numerical techniques are discussed. In addition, the chapters emphasize space science, space engineering, and plasmas and plasma processing of materials.

Rarefied Gas Dynamics: Experimental Techniques and Physical Systems

CONTENTS:
Experimental Diagnostics
Nonequilibrium Flows
Collision Phenomena
Rate Processes and Materials Processing
Clusters
Freejets
Shock Phenomena
Surface Science
Thermodynamic Studies
1994, 633 pp., illus, Hardback, ISBN 1-56347-079-9
AIAA Members: \$69.95, Nonmembers: \$99.95
Order #: V-158 (945)

Rarefied Gas Dynamics: Theory and Simulations

CONTENTS:
Discrete Velocity Models
Relaxation and Rate Processes
Direct Simulation Monte Carlo Method: Methodology
Direct Simulation Monte Carlo Method: Reactions and Flows
Mathematical Techniques
Discrete Lattice Methods and Simulations
Evaporation and Condensation
Kinetic Theory
Transport Processes
1994, 711 pp., illus, Hardback, ISBN 1-56347-080-2
AIAA Members: \$69.95, Nonmembers: \$99.95
Order #: V-159 (945)

Rarefied Gas Dynamics: Space Science and Engineering

CONTENTS:
Satellite Aerodynamics
Rarefied Aerodynamic Flows
Hypersonic Rarefied Flows
Plasma Physics
Transport Phenomena and Processes
1994, 545 pp., illus, Hardback, ISBN 1-56347-081-0
AIAA Members: \$69.95, Nonmembers: \$99.95
Order #: V-160 (945)

Place your order today! Call 1-800/682-AIAA



American Institute of Aeronautics and Astronautics

Publications Customer Service, 9 Jay Gould Ct., P.O. Box 753, Waldorf, MD 20604
FAX 301/843-0159 Phone 1-800/682-2422 8 a.m. - 5 p.m. Eastern

Sales Tax: CA residents, 8.25%; DC, 6%. For shipping and handling add \$4.75 for 1-4 books (call for rates for higher quantities). Orders under \$100.00 must be prepaid. Foreign orders must be prepaid and include a \$25.00 postal surcharge. Please allow 4 weeks for delivery. Prices are subject to change without notice. Returns will be accepted within 30 days. Non-U.S. residents are responsible for payment of any taxes required by their government.